

Constraints on Scalar Couplings from $\pi^\pm \rightarrow l^\pm \nu_l$

Bruce A. Campbell and David W. Maybury

Department of Physics, University of Alberta, Edmonton AB T6G 2J1, CANADA

Abstract

New interactions with Lorentz scalar structure, arising from physics beyond the standard model of electroweak interactions, will induce effective pseudoscalar interactions after renormalization by weak interaction loop corrections. Such induced pseudoscalar interactions are strongly constrained by data on $\pi^\pm \rightarrow l^\pm \nu_l$ decay. These limits on induced pseudoscalar interactions imply limits on the underlying fundamental scalar interactions that in many cases are substantially stronger than limits on scalar interactions from direct β -decay searches.

1 Introduction

While there is strong support for the $V - A$ form of the charged weak current, it is possible that new physics at or above the weak scale could give rise to scalar interactions that would compete with standard model processes. Examples of such possible physics include the exchange of extra Higgs multiplets which could enter the theory at scales from the Z mass upwards [1], leptoquarks which could be present at scales above 200 GeV [1], contact interactions from quark/lepton compositeness which could be present at the TeV scale [1], or strong gravitational interactions in TeV brane world models [1]. Recently, precision experiments [2, 3, 4] have searched for scalar interactions in β -decay, however, direct experimental constraints on scalar couplings still remain relatively weak as compared to the corresponding limits on pseudoscalar couplings [1, 5].

The precision of the limits on pseudoscalar couplings comes in part from the fact that the pion, a pseudoscalar meson, has a chirally suppressed decay $\pi^\pm \rightarrow l^\pm \nu_l$ which would be sensitive to new pseudoscalar interactions [6]. These pseudoscalar interactions would be detected by the failure of the standard model prediction [7] for the chiral suppression in the ratio of branching ratios $\frac{\Gamma(\pi^- \rightarrow e\bar{\nu})}{\Gamma(\pi^- \rightarrow \mu\bar{\nu})}$. It is the large chiral suppression factor, by the square of the electron/muon mass ratio, that allows such a powerful test of new physics that violates chirality and parity.

In the standard model, the leading contribution to pion decay occurs through tree level W exchange. At the quark level, this is the same process that is involved in the β -decay of a nucleon ignoring the spectator quarks. While the pion cannot decay through a scalar interaction, the pion can decay through induced pseudoscalar interactions generated from the electroweak renormalization of the scalar couplings. It is of considerable interest to use limits on the induced pseudoscalar couplings to set indirect limits on the size of the underlying scalar interactions.

In the following sections we outline our methods and estimate the limits on the size of scalar couplings based on the indirect effects from charged pion decay. We motivate the use of pion physics for constraining scalar interactions through discussion of a toy model.

This is followed by a more robust treatment where we use general operator techniques to obtain model independent results. Finally, we combined these results with data from pion decay and muon capture, to constrain the scalar couplings indirectly. We also discuss some of the implications of these results, and comment on prospects for future searches for scalar interactions.

2 Pion Physics and New Pseudoscalar Interactions

Consider constructing an effective Lagrangian and matrix element for the process $\pi^\pm \rightarrow l^\pm \nu_l$ in the presence of the pseudoscalar interactions. We can set limits on the strength of the pseudoscalar interactions from their interference with tree level W exchange. Since the pion is a pseudoscalar, we can use the following relations for current matrix elements,

$$\begin{aligned}
\langle 0 | \bar{u} \gamma_\mu \gamma_5 d | \pi(p) \rangle &= i\sqrt{2} f_\pi p_\mu \\
\langle 0 | \bar{u} \gamma_5 d | \pi(p) \rangle &= i\sqrt{2} \tilde{f}_\pi = i\sqrt{2} \frac{f_\pi m_\pi^2}{m_u + m_d} \\
\langle 0 | \bar{u} \sigma^{\mu\nu} \gamma_5 d | \pi(p) \rangle &= 0 \\
\langle 0 | \bar{u} \sigma^{\mu\nu} d | \pi(p) \rangle &= 0,
\end{aligned} \tag{1}$$

where $f_\pi = 93 \text{ MeV}$ and $\tilde{f}_\pi = 1.8 \times 10^5 \text{ MeV}^2$. The matrix element for the tree level W contribution can easily be constructed by using eq.(1), giving;

$$\mathcal{M}_{W^\pm} = G_F f_\pi \cos \theta_c [\bar{l} \gamma^\mu (1 - \gamma_5) \nu_l] p_\mu, \tag{2}$$

where p_μ is the pion momentum and θ_c is the Cabibbo angle. A pseudoscalar contribution with left-handed neutrinos in the final state can be expressed as a four-fermi contact operator,

$$\mathcal{L}_P = -i \frac{\rho}{2\Lambda^2} [\bar{l}(1 - \gamma_5) \nu_l] [\bar{u} \gamma_5 d] \tag{3}$$

where ρ is the pseudoscalar coupling constant. This expression can be converted to a matrix element using eq.(1),

$$\mathcal{M}_P = \rho \frac{\tilde{f}_\pi}{\sqrt{2}\Lambda^2} [\bar{l}(1 - \gamma_5) \nu_l]. \tag{4}$$

In the presence of a pseudoscalar interaction, the overall matrix element for the process $\pi^\pm \rightarrow l^\pm \nu_l$ is the coherent sum, $\mathcal{M}_P + \mathcal{M}_{W^\pm} = \mathcal{M}_l$.

$$\mathcal{M}_l = G_F f_\pi \cos \theta_c [\bar{l} \gamma^\mu (1 - \gamma_5) \nu_l] p_\mu + \frac{\rho \tilde{f}_\pi}{\sqrt{2} \Lambda^2} [\bar{l} (1 - \gamma_5) \nu_l] \quad (5)$$

Having constructed the matrix element, we can now estimate the ratio of branching ratios,

$$\frac{\Gamma(\pi^- \rightarrow e \nu_e)}{\Gamma(\pi^- \rightarrow \mu \nu_\mu)} = \frac{(m_\pi^2 - m_e^2) \langle |M_{e\nu}|^2 \rangle}{(m_\pi^2 - m_\mu^2) \langle |M_{\mu\nu}|^2 \rangle}. \quad (6)$$

Summing over final states of the squared matrix element we have

$$\begin{aligned} \langle |\mathcal{M}_l|^2 \rangle &= 4 G_F^2 f_\pi^2 \cos^2 \theta_c m_l^2 (m_\pi^2 - m_l^2) + 8 \frac{G_F \tilde{f}_\pi f_\pi \cos \theta_c \rho}{\sqrt{2} \Lambda^2} m_l (m_\pi^2 - m_l^2) \\ &\quad + 2 \frac{\rho^2 \tilde{f}_\pi^2}{\Lambda^4} (m_\pi^2 - m_l^2). \end{aligned} \quad (7)$$

For simplicity we have assumed that the pseudoscalar coupling is real, however, in general ρ may be complex. The more general expression is obtained by making the following replacements,

$$\begin{aligned} \rho &\rightarrow \frac{\rho + \rho^*}{2} = \text{Re}(\rho) \\ (\rho)^2 &\rightarrow |\rho|^2. \end{aligned} \quad (8)$$

We find that the branching ratio is given by

$$\frac{\Gamma(\pi^- \rightarrow e \nu_e)}{\Gamma(\pi^- \rightarrow \mu \nu_\mu)} = \frac{(m_\pi^2 - m_e^2)}{(m_\pi^2 - m_\mu^2)} \left[\frac{m_e^2 (m_\pi^2 - m_e^2) + R_e}{m_\mu^2 (m_\pi^2 - m_\mu^2) + R_\mu} \right], \quad (9)$$

where the $R_{e,\mu}$ functions are

$$R_{e,\mu} = \sqrt{2} \frac{\tilde{f}_\pi \text{Re}(\rho)}{G_F f_\pi \Lambda^2 \cos \theta_c} m_{e,\mu} (m_\pi^2 - m_{e,\mu}^2) + \frac{|\rho|^2 \tilde{f}_\pi^2}{2 f_\pi^2 G_F^2 \Lambda^4 \cos^2 \theta_c} (m_\pi^2 - m_{e,\mu}^2). \quad (10)$$

Thus far we have only discussed interactions with left-handed neutrinos in the final state. The inclusion of right-handed neutrinos requires a modification since pseudoscalar contributions to decays with right-handed neutrinos in the final state cannot interfere with the W exchange graph; hence the contributions to the rate add incoherently. With right-handed neutrinos, the expression for the matrix element becomes,

$$\mathcal{M}_P = \frac{\rho' \tilde{f}_\pi}{\sqrt{2} \Lambda^2} [\bar{l} (1 + \gamma_5) \nu_l], \quad (11)$$

where ρ' is the pseudoscalar coupling involving right-handed neutrinos. Defining

$$T \equiv \frac{(m_\pi^2 - m_e^2)^2 m_e^2}{(m_\pi^2 - m_\mu^2)^2 m_\mu^2} = 1.28 \times 10^{-4}, \quad (12)$$

we can express the branching ratio as

$$\frac{\Gamma(\pi^- \rightarrow e\nu_e)}{\Gamma(\pi^- \rightarrow \mu\nu_\mu)} = T \left(\frac{1 + \sqrt{2} \frac{\tilde{f}_\pi \text{Re}(\rho_e)}{G_F \Lambda^2 f_\pi \cos \theta_c m_e} + \frac{|\rho_e|^2 \tilde{f}_\pi^2}{2G_F^2 \Lambda^4 f_\pi^2 \cos^2 \theta_c m_e^2} + \frac{|\rho'_e|^2 \tilde{f}_\pi^2}{2G_F^2 f_\pi^2 \Lambda^4 \cos^2 \theta_c m_e^2}}{1 + \sqrt{2} \frac{\tilde{f}_\pi \text{Re}(\rho_\mu)}{G_F \Lambda^2 f_\pi \cos \theta_c m_\mu} + \frac{|\rho_\mu|^2 \tilde{f}_\pi^2}{2G_F^2 \Lambda^4 f_\pi^2 \cos^2 \theta_c m_\mu^2} + \frac{|\rho'_\mu|^2 \tilde{f}_\pi^2}{2G_F^2 \Lambda^4 f_\pi^2 \cos^2 \theta_c m_\mu^2}} \right) \quad (13)$$

If we assume either universal scalar couplings or else scalar couplings involving only the first generation, we obtain the following approximation for the ratio of decay widths,

$$\frac{\Gamma(\pi^- \rightarrow e\nu_e)}{\Gamma(\pi^- \rightarrow \mu\nu_\mu)} \approx T \left(1 + \sqrt{2} \frac{\tilde{f}_\pi \text{Re}(\rho)}{G_F \Lambda^2 f_\pi \cos \theta_c m_e} + \frac{|\rho|^2 \tilde{f}_\pi^2}{2G_F^2 \Lambda^4 f_\pi^2 \cos^2 \theta_c m_e^2} + \frac{|\rho'|^2 \tilde{f}_\pi^2}{2G_F^2 \Lambda^4 f_\pi^2 \cos^2 \theta_c m_e^2} \right) \quad (14)$$

We will discuss the effects of more general generation dependence of the scalar couplings in Section 6. The theoretical standard model calculation including radiative corrections is $\text{Br}_{\text{th}} = (1.2352 \pm .0005) \times 10^{-4}$ [7] and the measured experimental branching ratio is $\text{Br}_{\text{exp}} = (1.230 \pm .0040) \times 10^{-4}$ [1]. Saturating the experimental and theoretical uncertainty, we can obtain a bound on the pseudoscalar couplings,

$$\left| \sqrt{2} \frac{\tilde{f}_\pi \text{Re}(\rho)}{G_F \Lambda^2 f_\pi \cos \theta_c m_e} + \frac{|\rho|^2 \tilde{f}_\pi^2}{2G_F^2 \Lambda^4 f_\pi^2 \cos^2 \theta_c m_e^2} + \frac{|\rho'|^2 \tilde{f}_\pi^2}{2G_F^2 \Lambda^4 f_\pi^2 \cos^2 \theta_c m_e^2} \right| \leq 3 \times 10^{-3}. \quad (15)$$

3 Dressed W and Z Exchange with Scalar Fields: A Toy Theory

As an illustrative example of how an underlying scalar interaction induces an effective pseudoscalar interaction, it is useful to consider a toy theory where a VEVless scalar doublet is added to the standard model. In principle, the addition of a VEVless scalar doublet can lead to both scalar and pseudoscalar interactions in the tree level Lagrangian. Since the constraints on pseudoscalar interactions are already very strong from tree level contributions to

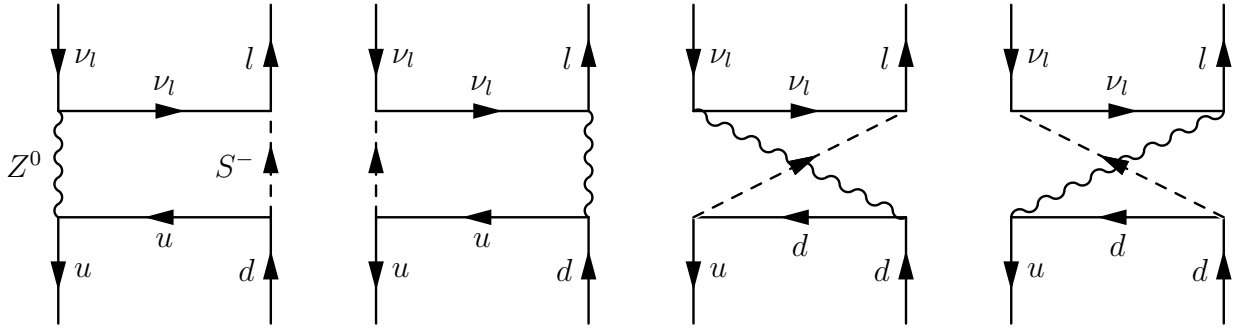


Figure 1: Dressed Z^0 exchange diagrams.

$\pi^\pm \rightarrow l^\pm \nu_l$ decay, and since we are interested in limits on pure scalar interactions, we arrange the couplings such that only scalar interactions arise at the scale of new physics,

$$\mathcal{L} = (\lambda) \bar{L} e_R S + (\lambda') \bar{Q} d_R S - (\lambda') \bar{Q} u_R \tilde{S} + \text{h.c.} \quad (16)$$

where, λ and λ' are the scalar couplings to the quarks and leptons respectively, and $\tilde{S} = i\sigma^2 S$.

In this working example, the scalar interactions have the property that they couple in a universal and flavour diagonal manner with undetermined scalar couplings to quarks and leptons. It is the charged scalar couplings that the β -decay experiments constrain directly. The pseudoscalar interaction can potentially be induced at one loop through three classes of diagrams: scalar-dressed Z exchanges, scalar-dressed W exchanges and vertex corrections (see Figure 1, Figure 2 and Figure 3). The weak interactions do not respect parity and the scalar interactions change chirality, thus diagrams of this form can potentially induce a pseudoscalar interaction.

To estimate the effect of the scalar on the branching ratio, we will make the approximation that the quarks are massless and ignore external momenta. Box diagrams that involve the Higgs or the Goldstone modes can be ignored since the couplings are mass proportional and hence their contribution is small. We start with the first class of diagrams, dressed Z exchange (see Figure 1). Summing the contributions of the four box diagrams in Figure 1,

working in the Feynman-'t Hooft gauge ($\xi = 1$), we obtain the following effective Lagrangian,

$$\begin{aligned}
\mathcal{L}_{S^-} = & \frac{ig^2(\lambda\lambda')}{32(4\pi)^2 \cos^2 \theta_w} F(M_s^2, M_Z^2) \left\{ [\bar{l}\gamma^\mu\gamma^\nu(1-\gamma_5)\nu_l][\bar{u}\gamma_\nu\gamma_\mu(1-\frac{8}{3}\sin^2\theta_w+\gamma_5)d] \right. \\
& + [\bar{l}\gamma^\mu\gamma^\nu(1-\gamma_5)\nu_l][\bar{u}\gamma_\mu\gamma_\nu(-1+\frac{4}{3}\sin^2\theta_w+\gamma_5)d] \\
& - [\bar{l}\gamma^\mu\gamma^\nu(1-4\sin^2\theta_w+\gamma_5)\nu_l][\bar{u}\gamma_\mu\gamma_\nu(1-\frac{8}{3}\sin^2\theta_w+\gamma_5)d] \\
& \left. - [\bar{l}\gamma^\mu\gamma^\nu(1-4\sin^2\theta_w+\gamma_5)\nu_l][\bar{u}\gamma_\nu\gamma_\mu(-1+\frac{4}{3}\sin^2\theta_w+\gamma_5)d] \right\}
\end{aligned} \tag{17}$$

where eq.(1) has been used. The function $F(M_s^2, M_Z^2)$ results from the loop integral. We can turn this into an expression for the amplitude for $\pi^\pm \rightarrow l^\pm \nu_l$ decay by using the identity

$$\gamma_\nu\gamma_\mu = \frac{\{\gamma_\nu, \gamma_\mu\}}{2} + \frac{[\gamma_\nu, \gamma_\mu]}{2} = -\frac{i}{2}\sigma_{\nu\mu} + g_{\nu\mu}, \tag{18}$$

and taking a matrix element between the vacuum and the on-shell pion state using eq.(1)

$$\begin{aligned}
\mathcal{M}_{S^-} = & \frac{-g^2\sqrt{2}\tilde{f}_\pi(\lambda\lambda')}{4(4\pi)^2 \cos^2 \theta_w} F(M_s^2, M_z^2) \\
& \left\{ [\bar{l}(1-\gamma_5)\nu_l] - [\bar{l}(1-\gamma_5)\nu_l] - [\bar{l}(1-4\sin^2\theta_w)\nu_l] + [\bar{l}(1-4\sin^2\theta_w)\nu_l] \right\} \\
= & 0.
\end{aligned} \tag{19}$$

This class of diagrams does not give a contribution.

We now consider the the second class of diagrams, the dressed W exchange class as seen in Figure 2. Again, we construct an effective Lagrangian for this process.

$$\begin{aligned}
\mathcal{L}_{S^0} = & -i\frac{g^2(\lambda\lambda')\cos\theta_c}{32M_W^2(4\pi)^2} F(M_s^2, M_w^2) \\
& \left\{ [\bar{l}\gamma^\nu\gamma^\mu(1-\gamma_5)d][\bar{u}\gamma_\mu\gamma_\nu(1+\gamma_5)d] + [\bar{l}\gamma^\nu\gamma^\mu(1-\gamma_5)d][\bar{u}\gamma_\nu\gamma_\mu(1-\gamma_5)d] \right\}
\end{aligned} \tag{20}$$

Taking a matrix element between the vacuum and one pion state as before, we find a vanishing amplitude

$$\begin{aligned}
\mathcal{M}_{S^0} = & -i\frac{g^2\sqrt{2}f_\pi(\lambda\lambda')\cos\theta_c}{32M_W^2(4\pi)^2} F(M_s^2, M_w^2) \left\{ [\bar{l}(1-\gamma_5)\nu_l] - [\bar{l}(1-\gamma_5)\nu_l] \right\} \\
= & 0.
\end{aligned} \tag{21}$$

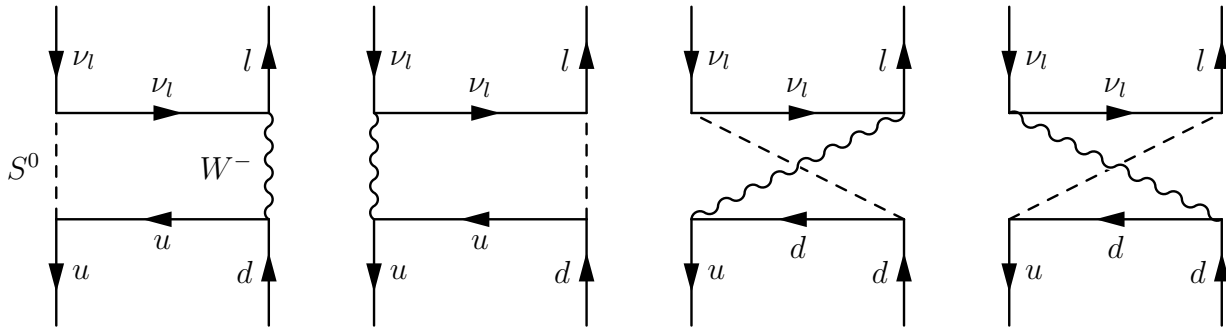


Figure 2: Dressed W exchange diagrams.

In this case, the cancellation came in part from the fact that the neutral scalar must couple to the up and down like quarks with a relative minus sign as dictated by weak isospin. The results from the first two classes of diagrams seem strange in that there is no symmetry protecting a pseudoscalar interaction from being induced. It should be noted that it is only the pseudoscalar part of the diagrams which appears in the matrix element constructed from the contraction with the on-shell pion state and the vacuum that cancels.

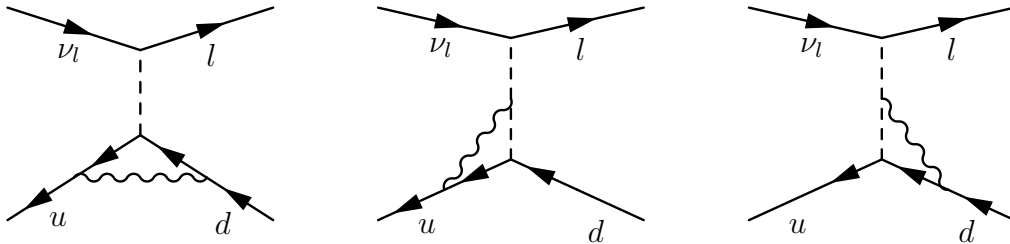


Figure 3: Radiative corrections to the quark-scalar vertex.

In the vertex correction class of diagrams we are dealing with primitively divergent graphs (see Figure 3). In order to get a conservative estimate of the induced pseudoscalar arising already from threshold effects, we can cut off the loop momentum at the weak scale and integrate from 0 to M_Z . In this case we find a non-vanishing contribution. The three graphs

in Figure 3 give the following result for the matrix element,

$$\mathcal{M}_T = -\frac{\sqrt{2}g^2\tilde{f}_\pi\lambda\lambda'}{64\pi^2\cos^2\theta_w M_Z^2} \left[\left(-\frac{4}{3}\sin^2\theta_w\right)\ln(2) + \cos(2\theta_w)\left(\ln(2) - \frac{1}{2}\right) \right] [\bar{l}(1 - \gamma_5)\nu_l] \quad (22)$$

Using eq.(15) in the absence of right-handed neutrinos, we find

$$\left| \frac{K_s}{G_F} \right| \leq 5 \times 10^{-3} \quad (23)$$

where,

$$|K_s| \equiv \frac{\lambda\lambda'}{M_Z^2}. \quad (24)$$

The above calculation gives a conservative estimate of the amplitude, including only contributions from threshold effects. To get an estimate of the growth of the induced pseudoscalar as we raise the scale of the scalar doublet mass above the electroweak scale, we can examine the beta functions of the theory. If we move to the chiral basis we see that there are two different couplings in the theory as shown in Figure 4. If we impose the condition that these

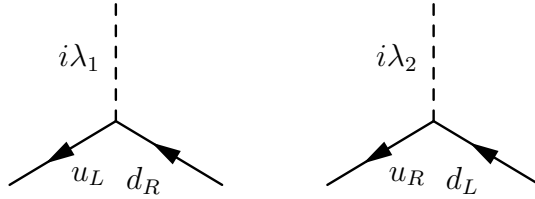


Figure 4: Scalar vertices written in the chiral basis. Note that if $\lambda_1 = \lambda_2$ the interaction is purely scalar.

two constants are equal at the scale of new physics, then the resulting interaction is parity invariant at that scale. This would mean the absence of any tree level pseudoscalar exchange. However, there is no conservation principle that would guarantee that the equality condition is met at all scales; the scalar vertex is renormalized. Since the weak interactions are not parity invariant, the beta functions for these two couplings are different. Therefore each of the two couplings in Figure 4 renormalize differently. Cutting off the loop momentum

at M_Z represents a conservative estimate, in that the scale of new physics is at the weak scale and therefore there is no scale separation for renormalization group running proper. We see in this toy example that even from threshold effects alone a pseudoscalar interaction will be radiatively induced. In order to quantitatively talk about the induced pseudoscalar, we need to examine the renormalization group equations for this interaction. This can be accomplished in a model independent way in the language of effective field theory, which we examine in the next section.

4 Local Scalar Operator Analysis

As mentioned in the last section, we expect a pseudoscalar interaction to be radiatively induced from a scalar interaction by weak interaction dressings. In order to consider this in a model independent manner, independent of the underlying physics responsible for the scalar interaction, we undertake an effective field theory operator analysis. Suppose that at some scale Λ there exists new physics that generates a purely scalar interaction. It may be due to fundamental scalars as in the toy theory in Section 3 or it may be due to a variety of other physics such as compositeness, extra dimensions, leptoquarks, etcetera. Independent of the details of the new physics that generates the scalar interactions, they will appear as non-renormalizable four-fermi scalar contact operators below the scale Λ . This allows us to examine this problem from the viewpoint of effective field theory.

In order to facilitate power counting, the $\overline{\text{MS}}$ scheme is most often used with effective field theory [8]. The $\overline{\text{MS}}$ scheme (or any mass independent subtraction scheme) presents the subtlety that heavy particles do not decouple in beta function calculations. That is, mass independent renormalization schemes do not satisfy the conditions of the Appelquist-Carazzone theorem [8]. This is dealt with by simply integrating out the heavy fields by hand at their associated scale. Thus whether we analyze the vertex corrections in a UV complete theory or in the effective theory, we will arrive at the same beta functions (up to threshold corrections) provided that we are only interested in results below Λ and only up to some finite power of $(\frac{1}{\Lambda})$.

We start by considering $SU(2) \times U(1)$ invariant four-fermion contact interactions that are generation independent and flavour diagonal (see Figure 5 and Figure 8). We will discuss the effects of generation dependence in Section 6. We consider two types of scalar operators in order to facilitate comparison with the direct experimental constraints. Type A (O_A) have left-handed neutrinos in the final state while Type B (O_B) have right-handed (sterile) neutrinos. These interactions appear as extensions to the standard model Lagrangian involving non-renormalizable operators,

$$\mathcal{L}_{\text{scalar}} = \frac{s_A}{\Lambda^2} O_A + \frac{s_B}{\Lambda^2} O_B \quad (25)$$

where s_A and s_B are undetermined scalar couplings. From these interactions, electroweak radiative corrections (see Figure 6 and Figure 9) can in principle induce pseudoscalar interactions. We retain corrections up to order $\frac{1}{\Lambda^2}$ and from this analysis we extract the anomalous dimension matrix.

4.1 Type A Operator Analysis: O_A

The operators of Type A are as follows,

$$O_1 = [\bar{e}_R L][\bar{Q} d_R] \quad (26)$$

$$O_2 = [\bar{e}_R L][\bar{u}_R Q], \quad (27)$$

(where the $SU(2)$ indices have been suppressed) such that the pure scalar interaction is

$$O_A = O_1 + O_2. \quad (28)$$

Since we are assuming that at the scale Λ there is a pure scalar interaction, we take O_1 and O_2 to enter the theory at the high scale with equal weight.

In calculating the anomalous dimension matrix a third operator is generated through renormalization: the operator $O' = [\bar{e}_R Q][\bar{u}_R L]$ mixes with the other two. However, in order to construct the matrix element for the pion decay amplitude, we need to rotate the operators to a basis that has a definite matrix element between the vacuum and the on-shell

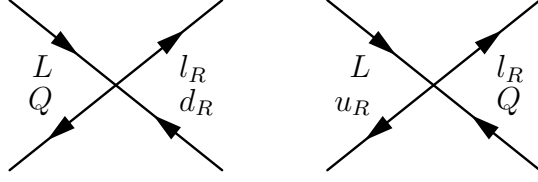


Figure 5: \mathcal{O}_1 and \mathcal{O}_2 , Type A contact interactions

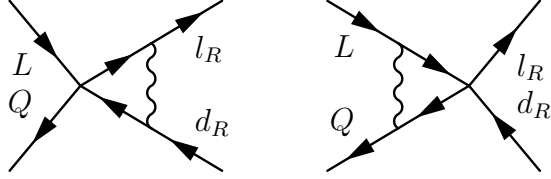


Figure 6: Example of electroweak corrections to Type A contact interactions. All permutations are required including wavefunction renormalization; the vector bosons are the $W_\mu^{1,2,3}$ and B_μ .

pion state. This requires Fierz reordering,

$$\mathcal{O}' = -\frac{1}{2}\mathcal{O}_2 + \left(-\frac{1}{8}\right)[\bar{e}_R\sigma_{\mu\nu}L][\bar{u}_R\sigma^{\mu\nu}Q] \quad (29)$$

where we define

$$\mathcal{O}_3 \equiv \left(-\frac{1}{8}\right)[\bar{e}_R\sigma_{\mu\nu}L][\bar{u}_R\sigma^{\mu\nu}Q]. \quad (30)$$

Note that $\langle 0|\mathcal{O}_3|\pi(p)\rangle = 0$. This leaves us with the following beta functions,

$$\mu\frac{\partial(\mathcal{O})}{\partial\mu} = \frac{1}{32\pi^2\Lambda^2}\gamma\mathcal{O} \quad (31)$$

where,

$$\mathcal{O} = \begin{pmatrix} \mathcal{O}_1 \\ \mathcal{O}_2 \\ \mathcal{O}_3 \end{pmatrix} \quad (32)$$

and

$$\gamma = \begin{bmatrix} 6g^2 + \frac{98}{9}g'^2 & 0 & 0 \\ 0 & 6g^2 + \frac{128}{9}g'^2 & 6g^2 + 10g'^2 \\ 0 & \frac{9}{2}g^2 + \frac{15}{2}g'^2 & 12g^2 + \frac{103}{9}g'^2 \end{bmatrix}. \quad (33)$$

The constants g' and g are the U(1) and SU(2) coupling constants, respectively. The results of the numerical integration of the renormalization group equations are displayed in Figure 7. O_1 and O_2 start out with equal amplitude at the scale Λ . They are then renormalized to the weak scale of roughly 100 GeV. In the first panel the x-axis indicates the starting scale Λ , i.e. the scale of new physics. The y-axis indicates the amount each operator is suppressed in running from the scale Λ to the weak scale. Each operator renormalizes differently and the splittings give rise to the pseudoscalar interaction. If the the scale Λ is at or very near the weak scale then threshold effects become important. We can roughly estimate the threshold effects to be at the level of eq.(23). Indeed it is only for a scalar doublet exchange that we need to consider a possible scale for new physics near the electroweak scale. For leptoquarks, compositeness, and extra dimensional gravity, direct experimental constraints imply that the scale Λ of new physics is sufficiently above the electroweak scale for RGE running to dominate threshold effects. The second panel plots the difference of O_1 and O_2 as a function of scale. This difference is proportional to the amount of pseudoscalar interaction induced.

4.2 Type B Operator Analysis: O_B

The Type B operators are as follows,

$$O_1 = [\bar{L}\nu_R][\bar{Q}d_R] \quad (34)$$

$$O_2 = [\bar{L}\nu_R][\bar{u}_RQ] \quad (35)$$

(where the SU(2) indices have been suppressed) with

$$O_B = O_1 + O_2. \quad (36)$$

We assume that the interaction at the scale Λ is purely scalar as in the Type A sce-

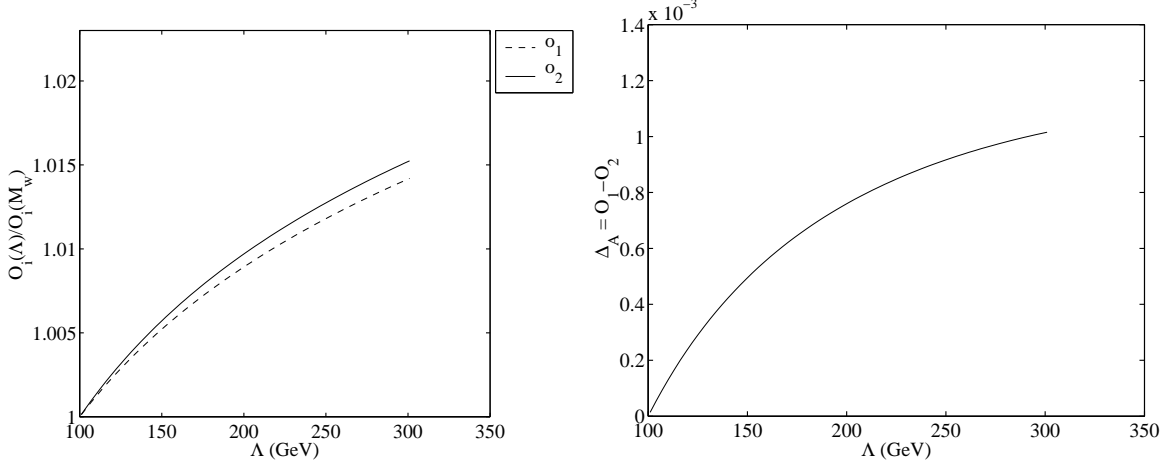


Figure 7: Type A operator RGE analysis. The first panel shows how each operator evolves with scale. The second panel displays the induced pseudoscalar proportionality factor.

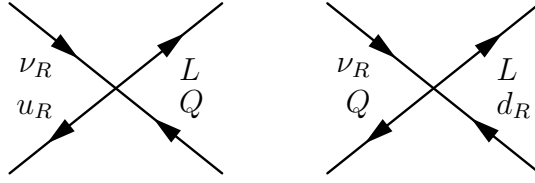


Figure 8: \mathcal{O}_1 and \mathcal{O}_2 , Type B contact interactions

nario. Again operator mixing is present with a third induced operator, namely $O' = [\bar{L}d_R][\bar{Q}\nu_R]$ which must be rotated as before into the appropriate basis: $O' = -\frac{1}{2}O_2 + (-\frac{1}{8})[\bar{L}\sigma^{\mu\nu}\nu_R][\bar{Q}\sigma_{\mu\nu}d_R]$ where $O_3 = (-\frac{1}{8})[\bar{L}\sigma^{\mu\nu}\nu_R][\bar{Q}\sigma_{\mu\nu}d_R]$. We extract the following anomalous dimension matrix:

$$\mu \frac{\partial(\mathcal{O})}{\partial\mu} = \frac{1}{32\pi^2\Lambda^2}\gamma\mathcal{O} \quad (37)$$

where,

$$\mathcal{O} = \begin{pmatrix} O_1 \\ O_2 \\ O_3 \end{pmatrix} \quad (38)$$

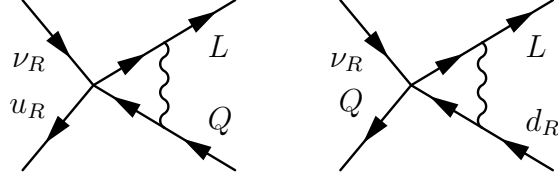


Figure 9: Example of electroweak corrections to Type B contact interactions. All permutations are required including wavefunction renormalization; the vector bosons are the $W_\mu^{1,2,3}$ and B_μ .

and

$$\gamma = \begin{bmatrix} 6g^2 + \frac{38}{9}g'^2 & 0 & 0 \\ 0 & 6g^2 + \frac{11}{9}g'^2 & 6g^2 - \frac{2}{3}g'^2 \\ 0 & \frac{9}{2}g^2 - \frac{1}{3}g'^2 & 12g^2 + \frac{34}{9}g'^2 \end{bmatrix}. \quad (39)$$

The results of the numerical integration of the renormalization group equations are displayed

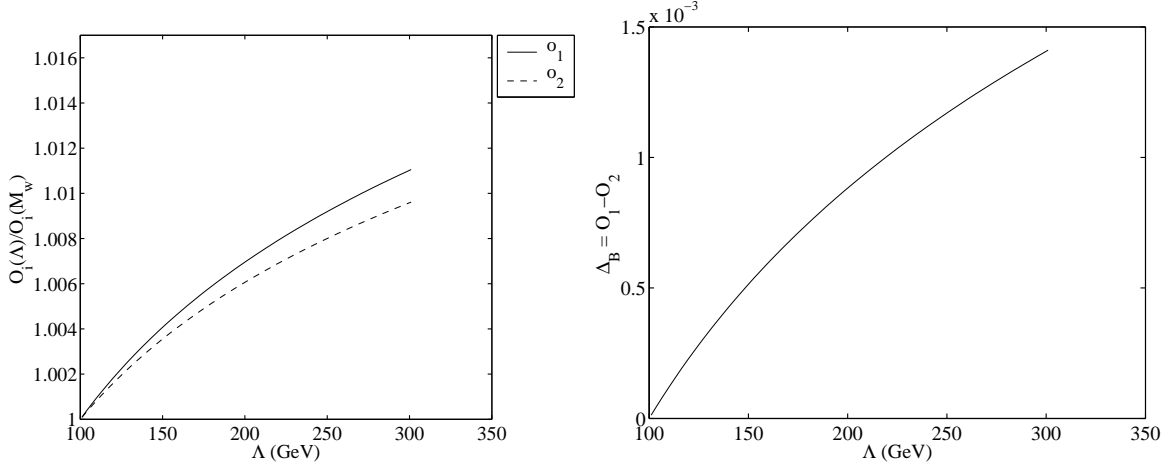


Figure 10: Type B operator RGE analysis. The first panel shows how each operator evolves with scale. The second panel displays the induced pseudoscalar proportionality factor.

in Figure 10. As we have seen before in Section 4.1 the graphs in Figure 10 illustrate the effects of renormalization on the operators O_1 and O_2 when they enter with the same amplitude at the scale Λ .

In both Type A and B scalar interactions we see that renormalization effects induce a pseudoscalar interaction. The size of the pseudoscalar interaction depends on how far the scale Λ is from the weak scale. The larger the scale separation is, the larger the induced pseudoscalar proportionality factor becomes. As noted above, even for the new scale Λ near the W and Z mass, we can estimate the size of the induced pseudoscalar from the threshold effects calculated in eq.(23). The effective pseudoscalar couplings, which we call ρ and ρ' as in Section 2, are given by,

$$\begin{aligned}\rho &= s_A \Delta_A(\Lambda) \\ \rho' &= s_B \Delta_B(\Lambda)\end{aligned}\tag{40}$$

where Δ_A and Δ_B are the renormalization group factors induced from the running from the scale Λ down to the weak scale (Δ_A and Δ_B are plotted in the second panel of Figure 7 and Figure 10). The factors s_A and s_B are the undetermined scalar coupling constants introduced in eq.(25). Since the pseudoscalar is induced from a scalar interaction we are now in a position to place limits on the magnitude of the scalar coupling from pion physics; the scalar couplings s_A and s_B at the scale of the new physics Λ are now constrained by the requirement that ρ and ρ' satisfy eq.(15).

A comment on QCD corrections is in order. QCD is a parity invariant theory and therefore QCD corrections cannot induce a pseudoscalar interaction by themselves. In our analysis, the induced pseudoscalar is coming from the difference of two operators that initially combined to give a purely scalar interaction and the QCD corrections will affect the two operators in the same way. The QCD corrections can only adjust this difference by an overall multiplicative factor. This is true for both operators of Type A and B. It is easy to estimate this correction. The largest part of the correction will come from QCD renormalization effects on the two operators from the weak scale down to the chiral symmetry breaking scale, of order $4\pi f_\pi \approx 1\text{GeV}$ [9], where we take the pion decay matrix element using PCAC. The correction to each of the operators can be computed through the QCD renormalization

group running of these operators,

$$\begin{aligned} O_{A,B}(1 \text{ GeV}) &= \left(\frac{\alpha_s(1 \text{ GeV}^2)}{\alpha_s(M_W^2)} \right)^{4/21} O_{A,B}(M_w) \\ &\approx 1.3 O_{A,B}(M_w) \end{aligned} \quad (41)$$

for $\Lambda_{QCD} = 200 \text{ MeV}$. The induced pseudoscalar, which is proportional to $\Delta_{A,B}$, will be enhanced by this factor of 1.3

5 Comparison with β -Decay Constraints

We can compare our bounds on scalar currents, with those arising in nuclear β -decay. The effective Hamiltonian for allowed β -decay has the general Lorentz form [10],

$$\begin{aligned} H &= \frac{G_F}{\sqrt{2}} \{ (\bar{\psi}_p \gamma_\mu \psi_n) (C_V \bar{\psi}_e \gamma_\mu \psi_\nu + C'_V \bar{\psi}_e \gamma_\mu \gamma_5 \psi_\nu) \\ &\quad + (\bar{\psi}_p \gamma_\mu \gamma_5 \psi_n) (C_A \bar{\psi}_e \gamma_\mu \psi_\nu + C'_A \bar{\psi}_e \gamma_\mu \gamma_5 \psi_\nu) \\ &\quad + (\psi_p \psi_n) (C_S \bar{\psi}_e \psi_\nu + C'_S \bar{\psi}_e \gamma_5 \psi_\nu) \\ &\quad + \frac{1}{2} (\bar{\psi}_p \sigma_{\lambda\mu} \psi_n) (C_T \bar{\psi}_e \sigma_{\lambda\mu} \psi_\nu + C'_T \bar{\psi}_e \sigma_{\lambda\mu} \gamma_5 \psi_\nu) \}. \end{aligned} \quad (42)$$

In the absence of right-handed currents, $C_i = C'_i$ and as we have mentioned before, we consider purely scalar interactions. (Note that in the above, $\frac{1+\gamma_5}{2}$ is taken to be the left projector. This is opposite to our convention in the preceding sections. However by using this convention in this section, it will be easier to compare with the β -decay literature.) The transition probability per unit time is given by [10],

$$w_{if} = \frac{\xi}{4\pi^3} p_e E_e (E_{max} - E_e) \left(1 + a v_e \cos \theta + b \frac{2m_e}{E_e} \right) \sin \theta d\theta \quad (43)$$

where E_{max} is the maximum energy of the electron in beta decay, $v_e = p_e/E_e$ and,

$$\begin{aligned} \xi &= \frac{1}{2} |M_F|^2 (|C_V|^2 + |C'_V|^2 + |C_S|^2 + |C'_S|^2) + \frac{1}{2} |M_{GT}|^2 (|C_A|^2 + |C'_A|^2 + |C_T|^2 + |C'_T|^2) \\ a\xi &= \frac{1}{2} |M_F|^2 (|C_V|^2 + |C'_V|^2 - |C_S|^2 - |C'_S|^2) - \frac{1}{6} |M_{GT}|^2 (|C_A|^2 + |C'_A|^2 - |C_T|^2 - |C'_T|^2) \\ b\xi &= \frac{1}{2} \text{Re} (C_S C_V^* + C'_S C_V'^*) |M_F|^2 + \frac{1}{2} \text{Re} (C_T C_A^* + C'_T C_A'^*) |M_{GT}|^2. \end{aligned} \quad (44)$$

The angle, θ , is the angle between the electron and neutrino momenta and b is the Fierz interference term. The parameter a has a simple form if we consider pure Fermi transitions $0^+ \rightarrow 0^+$. In this case the Gamow-Teller matrix elements are absent and the Fermi matrix elements divide out.

$$a = \frac{|C_V|^2 + |C'_V|^2 - |C_S|^2 - |C'_S|^2}{|C_V|^2 + |C'_V|^2 + |C_S|^2 + |C'_S|^2} \quad (45)$$

We see that if $a \neq 1$ then we have evidence for an effective scalar interaction. In the standard model $C_V = C'_V = 1$. We need to rewrite our expressions for scalar interactions in terms of \tilde{C}_s and \tilde{C}'_s where $\tilde{C}_i = C_i/C_V$. The scalar couplings can be re-expressed,

$$S_A = \frac{\Lambda^2 G_F \cos \theta_c}{\sqrt{2}} (\tilde{C}_s + \tilde{C}'_s) \quad (46)$$

$$S_B = \frac{\Lambda^2 G_F \cos \theta_c}{\sqrt{2}} (\tilde{C}_s - \tilde{C}'_s). \quad (47)$$

where in the equations in this section the interactions are all at the nucleon level. The operator analysis in Section 4 was completed with quarks, thus we need to include a scalar form factor to translate to the nucleon level. This form factor is on the order of 0.65 [11, 12]. So, the input nucleon level scalar coupling constants S_A and S_B are suppressed with respect to the quark level coupling constants s_A and s_B which we will bound, by this factor of order 0.65. The QCD correction is handled by multiplying the effective pseudoscalar couplings by the QCD enhancement factor before taking the pion matrix elements. From eq.(15) we see that the pion decay limits give the following constraint equation,

$$\left| 2 \frac{\tilde{f}_\pi \Delta_A}{f_\pi m_e} \text{Re}(\tilde{C}_s + \tilde{C}'_s) + \frac{\Delta_A^2 \tilde{f}_\pi^2}{f_\pi^2 m_e^2} |\tilde{C}_s + \tilde{C}'_s|^2 + \frac{\Delta_B^2 \tilde{f}_\pi^2}{f_\pi^2 m_e^2} |\tilde{C}_s - \tilde{C}'_s|^2 \right| \leq 3 \times 10^{-3} \quad (48)$$

where the scalar form factor and the QCD correction have been included. If we include only left-handed neutrinos in the theory, then we are constrained to lie along the line $\tilde{C}_s = \tilde{C}'_s$ whereas if we include only right-handed neutrinos we are forced to lie along $\tilde{C}_s = -\tilde{C}'_s$. We can now examine a few special cases.

In the absence of right-handed neutrinos, if we consider C_s and C'_s to be purely real and the scale Λ of the order of 200 GeV, the indirect limits from $\pi^\pm \rightarrow l^\pm \nu_l$ decay give us the limit

$$|\text{Re}(\tilde{C}_s)| = |\tilde{C}_s| \leq 2.5 \times 10^{-4}. \quad (49)$$

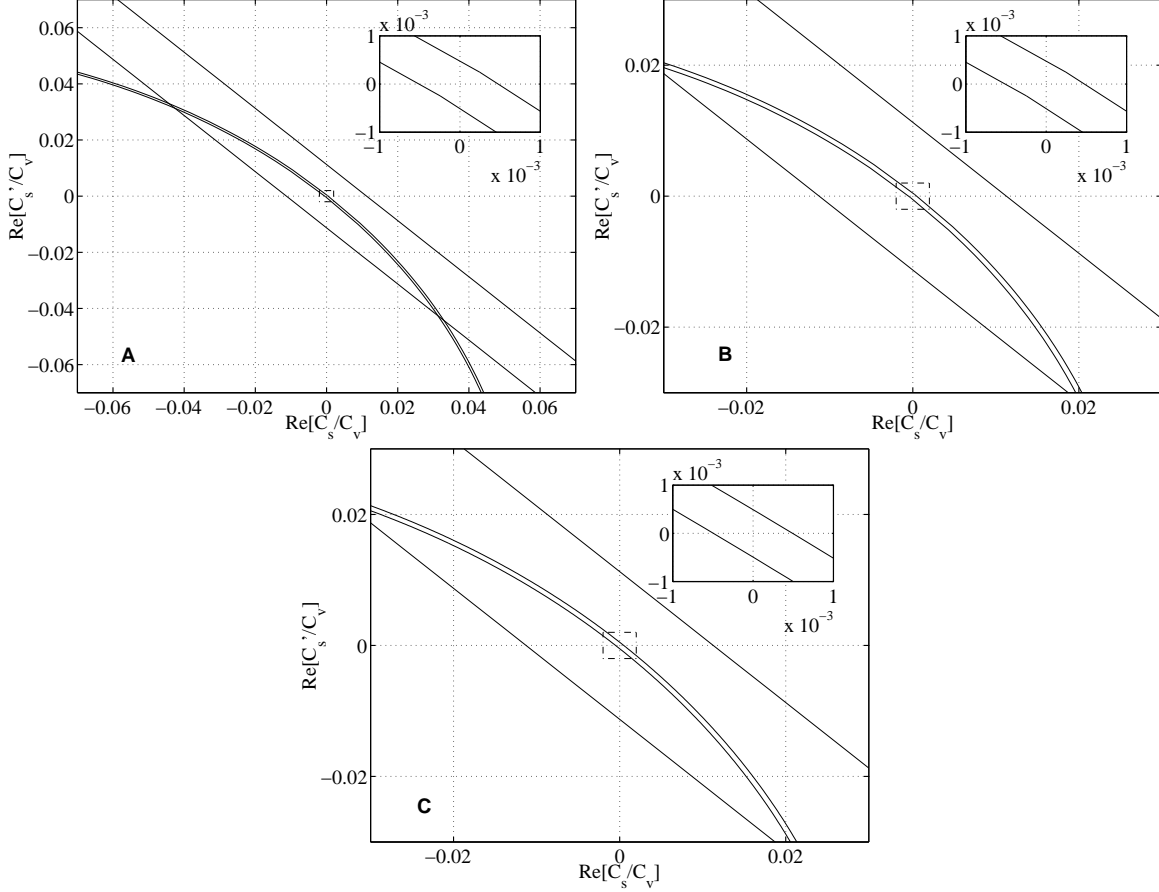


Figure 11: Constraint plots on the real parts of \tilde{C}_s and \tilde{C}'_s at $\Lambda = 200$ GeV. Panel A corresponds to a phase of 0° ; panel B to $\pm 45^\circ$; and panel C to 45° and -45° for \tilde{C}_s and \tilde{C}'_s respectively. The diagonal band is the experimental limit set by the b-Fierz interference term from β -decay. In all cases, the allowed region is the band between the two ellipses. The enlarged area more clearly shows the width of the region.

For comparison, the experimental 90% confidence limit determined from the b-Fierz interference term in β -decay (see eq.(44)) is $|\text{Re}(\tilde{C}_s)| \leq 8 \times 10^{-3}$ [3, 5]. We see that the indirect limit from pion decay is stronger by over an order of magnitude. On the other hand, if we consider C_s and C'_s to be purely imaginary; again in the limit of left-handed couplings we obtain,

$$|\text{Im}(\tilde{C}_s)| = |\tilde{C}_s| \leq 9.2 \times 10^{-3} \quad (50)$$

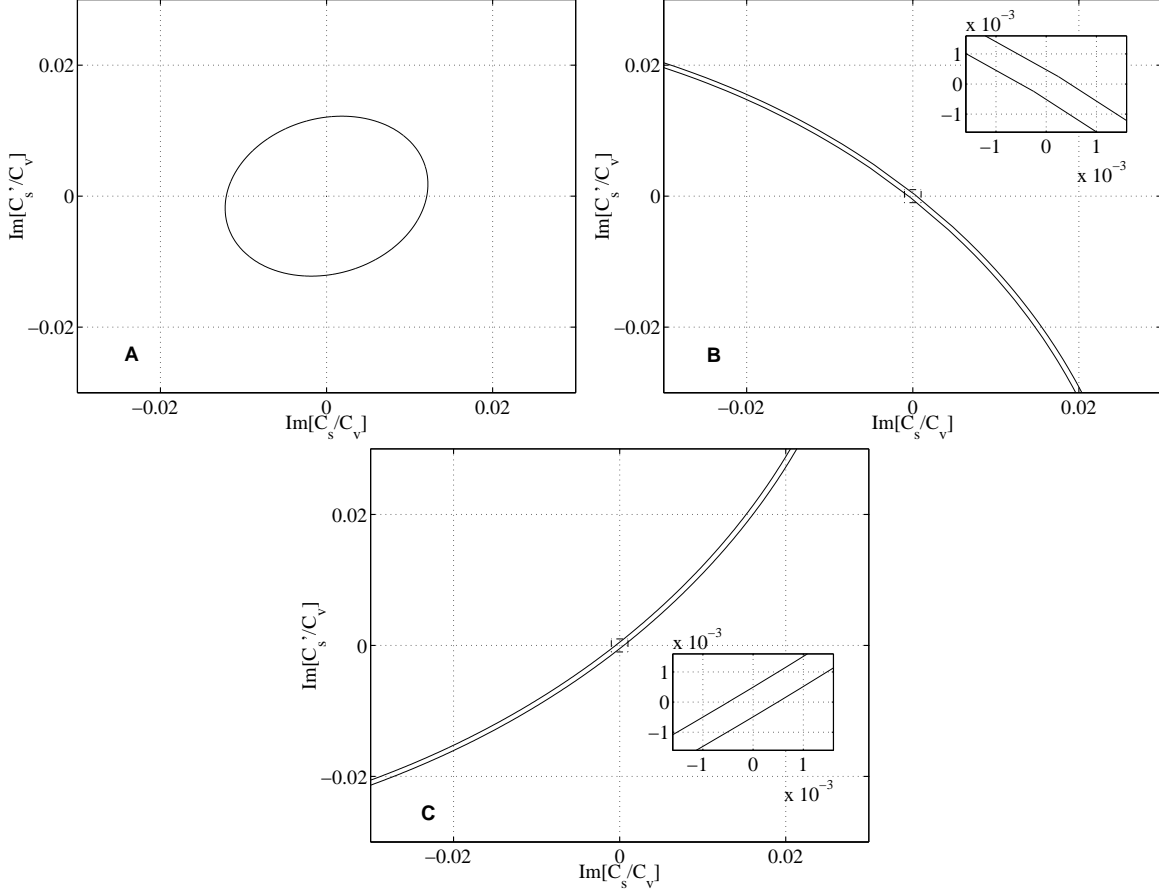


Figure 12: Constraint plots on the imaginary parts of \tilde{C}_s and \tilde{C}'_s at $\Lambda = 200$ GeV. Panel A corresponds to a phase of $\pm 90^\circ$; panel B to $\pm 45^\circ$; and panel C to 45° and -45° for \tilde{C}_s and \tilde{C}'_s respectively. In panel A, the interior of the ellipse is the constraint. In the remaining plots, the allowed region is the band between the two ellipses. The enlarged area more clearly shows the width of the region.

where the scale Λ is of the order of 200 GeV. Again for comparison, the experimental limit on the size of the imaginary part at the 95% confidence level, with only left-handed neutrinos, is approximately $|\text{Im}(\tilde{C}_s)| \leq 1 \times 10^{-1}$ [3]. The indirect $\pi^\pm \rightarrow l^\pm \nu_l$ limit is stronger by two orders of magnitude.

If we take $\tilde{C}_s = -\tilde{C}'_s$ so that we are in the limit of right-handed couplings and the b-Fierz

interference term vanishes we find,

$$|\tilde{C}_s| \leq 7.9 \times 10^{-3} \quad (51)$$

Again for comparison, at 1σ , the direct experimental constraint is $|\tilde{C}_s| \leq 6 \times 10^{-2}$ [3].

The limits presented here are in the case that the scale Λ was set to 200 GeV. Because the pseudoscalar interactions are induced by renormalization from Λ down to the electroweak scale, the higher the scale of new physics is, the more competitive our results become relative to beta decay. As the scale of new physics is lowered the constraints from $\pi^\pm \rightarrow l^\pm \nu_l$ become less stringent. However even in the worst case limit where the new scale is at the Z-mass and therefore we would no longer have an interval of renormalization group running, the renormalization threshold effects calculated in eq.(23) are still competitive. As an example, if we take C_s and C'_s to be real and ignore right-handed neutrinos we find that,

$$|\text{Re}(\tilde{C}_s)| = |\tilde{C}_s| \leq 3.5 \times 10^{-3}. \quad (52)$$

Plots of the pion physics constraints for the more general situation (where the real and imaginary parts of C_s and C'_s vary independently) are given in Figure 11 and Figure 12. We plot the constraints for the real and imaginary parts separately. Note from eq.(48) that the phases of C_s and C'_s are important when constructing these separate plots. In order to convey the effects of the phases most clearly, we have chosen three interesting cases. In the real plots we consider: C_s and C'_s to each have a phase of 0° ; C_s and C'_s to each have a phase of $\pm 45^\circ$; and the situation where C_s has a phase of 45° and C'_s has a phase of -45° . In the imaginary plots we consider: C_s and C'_s to each have a phase of $\pm 90^\circ$; C_s and C'_s each have a phase of $\pm 45^\circ$; and the case where C_s has a phase of 45° and C'_s has a phase of -45° . All three plots in the imaginary case are well within the region allowed by the direct experimental bounds [3, 13]. It is interesting to note that in the limit of sufficiently large phases (i.e. $> 85^\circ$) the ellipse bound in Figure 11 moves entirely inside the b-Fierz interference limit allowed region. This is expected since phases approaching 90° imply that C_s and C'_s are almost completely imaginary. When this situation occurs and we are in the limit of left-handed couplings (i.e. along the line $C_s = C'_s$), there are two solutions consistent with

the pion physics constraints and the b-Fierz interference bound. One solution is centered on 0 and the other is centered off 0 along the line $C_s = C'_s$ yet inside the b-Fierz interference limits. Even in these cases, the width of the ellipse bound is still of the order of 5×10^{-4} .

6 Comment on Flavour Dependent Couplings

Thus far we have obtained limits on scalar interactions in the limit of universal flavour couplings. Let us now relax this assumption. One case that deserves attention is the limit of mass proportional couplings. This implies that $R_e/(m_e^2(m_\pi^2 - m_e^2)) = R_\mu/(m_\mu^2(m_\pi^2 - m_\mu^2))$ in eq.(10) and therefore there is no effect on the pion branching ratio,

$$\begin{aligned} \frac{\Gamma(\pi^- \rightarrow e\nu_e)}{\Gamma(\pi^- \rightarrow \mu\nu_\mu)} &= \frac{(m_\pi^2 - m_e^2)}{(m_\pi^2 - m_\mu^2)} \left[\frac{m_e^2(m_\pi^2 - m_e^2) + S_e}{m_\mu^2(m_\pi^2 - m_\mu^2) + S_\mu} \right] \\ &= T. \end{aligned} \quad (53)$$

This observation also holds in the presence of right-handed neutrinos. However, in this case, we still can bound the scalar couplings involved in β -decay by combining the $\pi^\pm \rightarrow l^\pm \nu_l$ limits with data from muon capture experiments. Recent experiments and analysis of muon capture on ${}^3\text{He}$ indicate that the muon-nucleon scalar coupling is bounded by [14]

$$\frac{|S_\mu|}{\Lambda^2} \leq 4 \times 10^{-2} G_F \quad (54)$$

with a neutrino of left-handed chirality. Therefore, in the limit of mass proportional couplings, S_e/Λ^2 must be of the order of 200 times smaller due to the electron-muon mass ratio. This implies that \tilde{C}_s is bounded,

$$|\tilde{C}_s| \leq 2 \times 10^{-4}. \quad (55)$$

In order to estimate the degree to which the presence of muon scalar interactions can weaken the limits that we infer from $\pi^\pm \rightarrow l^\pm \nu_l$, let us assume that the muon scalar coupling saturates the experimental bound eq.(54). Substituting this into the expression for the pion branching ratio eq.(13), ignoring right-handed neutrinos and assuming a scale Λ of 200 Gev, eq.(15) is modified to the following form,

$$\left| \sqrt{2} \frac{\tilde{f}_\pi \text{Re}(\rho)}{G_F \Lambda^2 f_\pi \cos \theta_c m_e} + \frac{|\rho|^2 \tilde{f}_\pi^2}{2G_F^2 \Lambda^4 f_\pi^2 \cos^2 \theta_c m_e^2} \right| \leq 1 \times 10^{-2}. \quad (56)$$

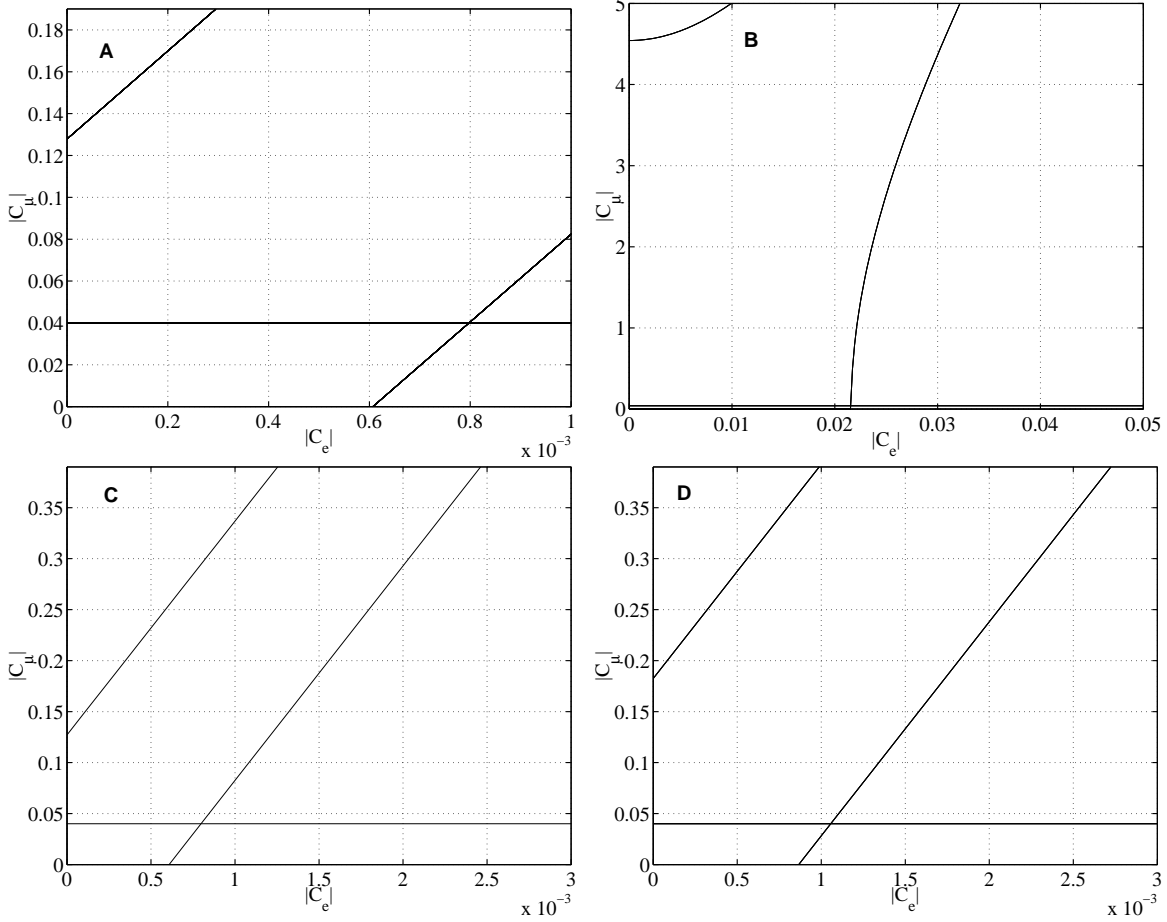


Figure 13: Constraint plots on the $|C_e|$ and $|C_\mu|$ couplings at $\Lambda = 200$ GeV. Panel A corresponds to phases for C_e and C_μ of $0^\circ, 0^\circ$; panel B to $90^\circ, 90^\circ$; panel C to $180^\circ, 180^\circ$; panel D to $\pm 45^\circ, \pm 45^\circ$ respectively. The allowed region is the interior of the band in each panel and below the horizontal line set by muon capture data.

We find this conservative approach has the effect of weakening our limits a factor of three at most compared to the analysis in Section 5. The limits on scalar couplings with $\Lambda = 200$ GeV, from $\pi^\pm \rightarrow l^\pm \nu_l$, combined with muon capture scalar limits, are substantially stronger than limits on scalar couplings from direct β -decay searches.

Finally, we consider the allowed region for the electron-scalar and muon-scalar couplings

in a model independent manner. Again the constraint equation derived from eq.(13) is,

$$\left| \left(\frac{1 + \sqrt{2} \frac{\tilde{f}_\pi \text{Re}(C_e) \Delta_A}{f_\pi \cos \theta_c m_e} + \frac{|C_e|^2 \Delta_A^2 \tilde{f}_\pi^2}{2 f_\pi^2 \cos^2 \theta_c m_e^2}}{1 + \sqrt{2} \frac{\tilde{f}_\pi \text{Re}(C_\mu) \Delta_A}{f_\pi \cos \theta_c m_\mu} + \frac{|C_\mu|^2 \Delta_A^2 \tilde{f}_\pi^2}{2 f_\pi^2 \cos^2 \theta_c m_\mu^2}} - 1 \right) \right| \leq 3 \times 10^{-3}, \quad (57)$$

where,

$$C_\mu = \frac{S_\mu}{G_F \Lambda^2} \quad C_e = \frac{S_e}{G_F \Lambda^2}. \quad (58)$$

We display the results in Figure 13 for a number of different phase conditions. We consider the cases where the complex phase of C_e and C_μ are $0^\circ, 0^\circ; 90^\circ, 90^\circ; 180^\circ, 180^\circ; \pm 45^\circ, \pm 45^\circ$, respectively.

7 Discussion

By considering renormalization effects on universal (or alternatively first generation), and flavour diagonal scalar operators, we have derived limits on the size of the ratio between scalar and vector couplings from precision measurements of $\pi^\pm \rightarrow l^\pm \nu_l$ decay. As a typical constraint value, in the absence right-handed neutrinos, we find that $|\text{Re}(\tilde{C}_s)| < 2.5 \times 10^{-4}$ for Λ of the order of 200 GeV. A more general comparison with the β -decay experiments (with the inclusion of right-handed neutrinos) is made in the plots in Figure 11 and Figure 12. We note that the most conservative estimate of the limits occurs when the new physics arises at the electroweak scale. In this case, the contribution to the induced pseudoscalar comes entirely from threshold corrections which we estimate from the model calculation in Section 3. The limit for real couplings in the absence of right-handed neutrinos from threshold contributions is $|\text{Re}(\tilde{C}_s)| < 3.5 \times 10^{-3}$. In the scenario where we have arbitrary generation dependence of the scalar couplings, $\pi^\pm \rightarrow l^\pm \nu_l$ limits can be combined with limits on scalar interactions in muon capture to bound the first generation scalar couplings. These limits are illustrated in particular cases in Figure 13.

These observations have implications for current β -decay experiments. Direct searches for scalar interactions in β -decay will be most competitive if the new physics responsible for the effective scalar interactions arises at the electroweak scale in the explicit exchange of

new scalars. In these circumstances, the indirect limits from threshold induced pseudoscalar interactions, eq.(52), are comparable to the direct β -decay scalar searches. For other choices of phase, the indirect limits from threshold effects can be weaker than the direct experimental constraints. Therefore, interest in searches for new scalar interactions with β -decay experiments remains undiminished.

On the other hand, for new effective scalar interactions arising as effective $SU(2) \times U(1)$ invariant operators at mass scales above 200 GeV (as expected in models with leptoquarks, composite quarks/leptons, or low scale quantum gravity) the constraints arising from the precision measurements of $\pi^\pm \rightarrow l^\pm \nu_l$ decay, combined with limits on scalar interactions in muon capture, can be stronger by an order of magnitude or more than the direct experimental searches. Furthermore, the relative strength of these searches becomes better, the higher the mass scale of the new physics is compared to the electroweak scale. This argues strongly for improved experimental precision in measurements of muon capture, and $\pi^\pm \rightarrow l^\pm \nu_l$ decay. In particular we note that in the case of pion decay, the experimental error exceeds the uncertainty in the theoretical calculation by a factor of eight. A new measurement of $\pi^\pm \rightarrow l^\pm \nu_l$ decay with an order of magnitude greater precision would not only constrain physics beyond the standard model which could potentially contribute to tree level pion decay, but as we have argued above, will also indirectly provide tests of new scalar interactions of unparalleled precision.

8 Acknowledgements

We would like to thank Eric Adelberger and John Behr for their generous assistance at several stages of this project. We have benefitted from useful discussions with John Ellis, Andrzej Czarnecki, Aneesh Manohar, Michael Luke, and Doug Bryman. We wish to thank J.P. Archambault and David Shaw for their help with the Feynmf package. This work was supported by the Natural Sciences and Engineering Research Council of Canada.

References

- [1] Particle Data Group, Phys. Rev. **D66**,(2002),
- [2] A. Garcia *et al.*, nucl-ex/9904001.
- [3] E. G. Adelberger *et al.* (ISOLDE), Phys. Rev. Lett. **83**, 1299 (1999), nucl-ex/9903002.
- [4] E. G. Adelberger, Phys. Rev. Lett. **70**, 2856 (1993).
- [5] For a review see: I. S. Towner and J. C. Hardy, nucl-th/9504015.
- [6] For a review see: D. A. Bryman Comments Nucl. Part. Phys. **21** 101 (1993).
- [7] W. J. Marciano and A. Sirlin, Phys. Rev. Lett. **71**, 3629 (1993).
- [8] For a review see: A. Manohar, hep-ph/9606222.
- [9] S. Weinberg, Physica **96A**, 327-340 (1979).
- [10] J. Jackson, S. Treiman, and H. Wyld Jr., Nucl. Phys. **4**, 206 (1957).
- [11] J. Behr: private communication. (2001).
- [12] K. F. Liu *et al.*, Phys. Rev. **D59**, 112001 (1999), hep-ph/9806491.
- [13] M. B. Schneider *et al.*, Phys. Rev. Lett. **51**, 1239 (1983).
- [14] J. Govaerts and J.-L. Lucio-Martinez, Nucl. Phys. **A678**, 110 (2000), nucl-th/0004056.